Materials Research Proceedings 28 (2023) 1235-1244 https://doi.org/10.21741/9781644902479-134

Orthogonal cutting with additively manufactured grooving inserts made from HS6-5-3-8 high-speed steel

KELLIGER Tobias[1,a *], MEURER Markus[1,b] and BERGS Thomas.[1,2,c]

[1]Laboratory for Machine Tools and Production Engineering (WZL) of RWTH Aachen University, Campus-Boulevard 30, 52074 Aachen, Germany

[2]Fraunhofer Institute for Production Technology (IPT), Steinbachstr. 17, 52074 Aachen, Germany

[a]t.kelliger@wzl.rwth-aachen.de, [b]M.Meurer@wzl.rwth-aachen.de, [c]t.bergs@wzl.rwth-aachen.de

Keywords: Orthogonal Cutting, Chip Formation, Additive Manufacturing, LPBF, HSS, ASP 2030, HS6-5-3-8

Abstract. Additive manufacturing (AM) of cutting materials such as high-speed steel (HSS) is very challenging. So far, the impact of the layer-by-layer manufacturing technique onto the AM tool performance during machining is widely unknown. In this study, the performance characteristics of AM grooving inserts manufactured from HS6-5-3-8 (ASP 2030) in AM Laser Powder Bed Fusion (LPBF) process were investigated in fundamental cutting experiments. Six different workpiece materials were analyzed and two different parameter sets for the LPBF process investigated. All AM grooving inserts withstood the thermal and mechanical stresses during machining of the investigated materials. Based on these results, AM threading tools manufactured from HS6-5-3-8 will be investigated in a next step, using the geometrical freedom of the AM process for an adapted channel and outlet nozzle design of the internal cutting fluid supply.

Introduction

Additively manufactured (AM) cutting tools enable new design concepts in tool development including benefits such as lightweight construction [1], damping behavior [2] and internal cutting fluid supply [3]. So far, mainly basic bodies of indexable cutting tools were additively manufactured from steel materials, with conventional cutting inserts mounted. AM tools such as drills, grooving toolholders or indexable milling tools can be already found in industrial applications [4-6]. AM processing of cutting materials is rather rare due to the high requirements to geometrical accuracy, defect-free production and the high demands for the material regarding thermal and mechanical resistance in use. Even though some studies dealing with the processing of cutting materials in different AM techniques exist, only very few works investigating the performance behavior of AM processed cutting tools during machining are known. Examples for AM cutting materials can be found in processing of tungsten-carbide in Binder Jetting [7], slurry-based three-dimensional printing (3DP) technology [8] as well as in Laser Powder Bed Fusion (LPBF) [9], processing of ceramics in Lithography-based Ceramic-Manufacturing (LCM) [10] or LPBF processing of HSS [11].

High-speed steel (HSS) still is a very relevant cutting material. Due to its favorable characteristics of high ductility and bending strength, HSS is widely used for drilling and threading tools but also in broaching of difficult-to-cut high-temperature resistant materials, fine blanking tools and high-performance bearings. [12]

LPBF (also known as SLM or DMLS) is the most commonly used AM technique [13]. Due to LPBF machine concepts with preheated base plate, processing of HSS materials became possible during the last years. Thus, even in hard-to-weld materials with high carbon content, such as HSS, crack formation can be prevented. Kempen et al. [14] manufactured AISI M2 HSS with a relative

density of 99.8 % and a hardness of 57 HRC. Zumofen et al. [15] used higher preheating temperatures to further reduce residual stresses in processing of AISI M2 HSS. Saewe et al. [11] processed defect-free AISI M50 HSS with a relative density up to 99.5 % and a hardness of up to 65 HRC for the application in roller bearings.

So far, no studies regarding the performance behavior of LPBF-processed HSS cutting materials in machining experiments are known. In this work, as-built grooving inserts manufactured from HS6-5-3-8 (ASP 2030) were investigated in orthogonal cutting experiments. Main evaluation criteria were cutting force components, tool wear and chip form. Thus, the potential of the AM HSS for an application in geometrical adapted AM threading tools with individualized cutting fluid supply should be assessed.

Tool Characteristics

In a first step, grooving insert test specimens were additively manufactured by LPBF from HS6-5-3-8 on a modified machine Aconity Midi at Fraunhofer Institute for Laser Technology (ILT). The cutting edges had a slight allowance for the downstream grinding process. Two different LPBF parameter settings were applied with focus on high density (Standard, relative density of 99.96 %) and high productivity (Productive, relative density of 99.87 %), see Fig. 1. As the inserts with a total height of 26 mm were built vertically, a slight increase of hardness between +3.2 % to +4.9 % could be detected between edge 1 close to the build plate and edge 2 in distance to the build plate. The hardness of the specimens built with the parameter setting Standard was around 24 % higher than for the parameter setting Productive. This can be explained by the longer exposure time of the laser per area and the resulting differences in heat generation and dissipation. As no heat-treatment was carried out, this difference in mechanical properties had to be considered for the machining experiments.

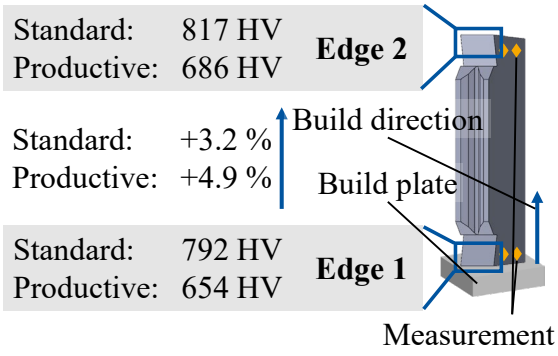

LPBF parameter settings

		Standard	Productive
Laser power	P_L / W	250	300
Scan speed	v_s / mm/s	940	1340
Hatch distance	Δy / µm	80	100
Layer thickness	D_s / µm	30	
Preheating	T / °C	350	

Fig. 1. Micro hardness measurement in dependency of build height and LPBF process parameters.

Both cutting edges of all inserts were then uniformly grinded by the company Meyer + Dörner Räumwerkzeuge GmbH. The cutting edges were measured on an optical microscope Algona Mikro CAD (cutting edge radius r_β) and a tactile contour measurement device MarSurf PCV (rake angle γ and clearance angle α). The mean values are given in Fig. 2, a. The tools were uncoated.

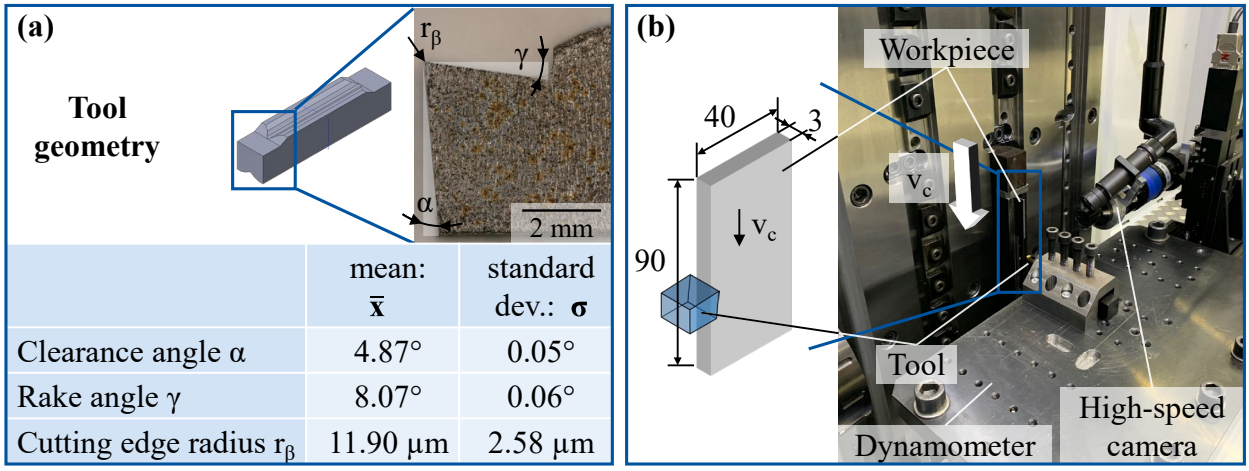

	mean: $\bar{x}$	standard dev.: σ
Clearance angle α	4.87°	0.05°
Rake angle γ	8.07°	0.06°
Cutting edge radius r_β	11.90 µm	2.58 µm

Fig. 2. Measured tool geometry over all investigated cutting edges (a) and experimental setup (b).

Experimental Setup

The experimental setup inside an external vertical broaching machine Forst RASX 2200x800x600 M / CNC is shown in Fig. 2, b. The tool holder was mounted on a dynamometer Kistler Z21289 on the machine table. The workpiece was clamped into the broaching stroke. The chip formation was captured with a high-speed camera Vision Research Phantom v7.3. In order to evaluate the performance behavior of the AM tools, chip formation, chip shape, cutting force and tool wear were investigated. Six different workpiece materials were analyzed with different cutting speed v_c and undeformed chip thickness h each. The cutting parameters are given in Table **1**. The applied materials were two steel alloys (X5CrNiMo17-12-2 (1.4401) and 42CrMo4+QT), one copper alloy (CuZn21Si3P (Ecobrass)), one cast iron (GJL 250) as well as two difficult-to-cut materials (Ti6Al4V (β-annealed) and Inconel 718).

Table 1. Cutting parameters for all investigated workpiece materials.

Workpiece material	v_c [m/min]	h [mm]
42CrMo4+QT	30	0.15
X5CrNiMo17-12-2 (1.4401)	30	0.15
CuZn21Si3P	60	0.2
GJL 250	60	0.2
Ti6Al4V	15	0.1
Inconel 718	5	0.05

For the evaluation of the force signal, cutting force F_c and cutting normal force F_{cN} (respective thrust force) were averaged within the range from 30 % to 70 % of the total signal of one cut (see Fig. 3). Each insert was only used for nine consecutive cuts within one workpiece material. Tool wear was analyzed by optical light microscopy and optical 3D measurement Alicona FocusG5.

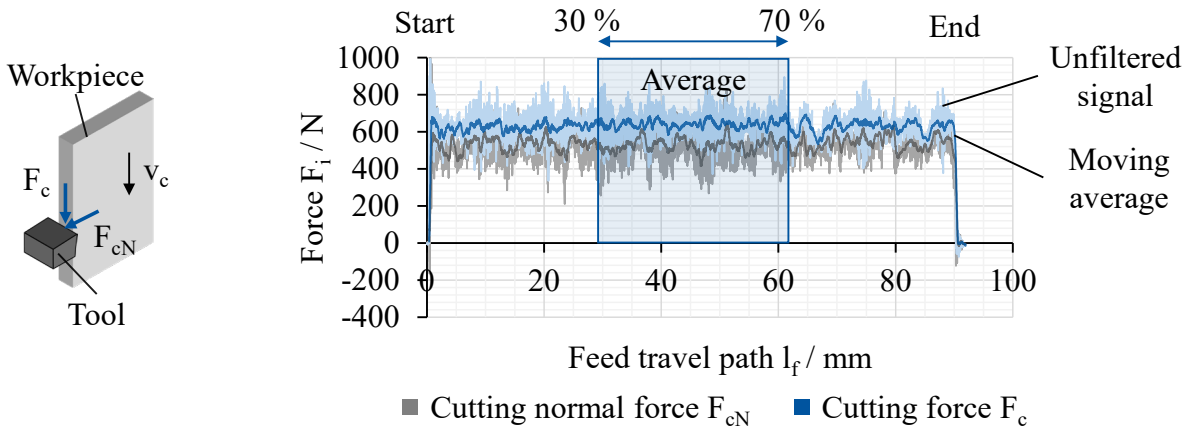

Fig. 3. Evaluation of force signal.

Results and Discussion

In the following section, different comparisons are made in order to evaluate influencing factors onto the tool performance within the scope of the experiments. Not all inserts were tested in each combination of edge number, LPBF parameter setting and workpiece material. A comparison between different materials is not useful as every material was machined with individual cutting parameters. The focus of the analysis was on the comparison between built height and LPBF parameter settings as well as on information regarding the performance behavior of the AM inserts in use with a wide range of different workpiece materials.

In Fig. 4 the influence of the build height (edge 1 and 2) onto the force development is shown for cutting of 42CrMo4 and Inconel 718 with inserts “Standard”. A significant change of the force amplitudes between cut no. 1 and no. 2 to 9 was observed for all experiments. This can be traced back to inaccuracies in the positioning of the machine table and thus the cutting edge relative to the workpiece surface for the first cut, leading to a slightly deviating undeformed chip thickness. For all following analyses, the mean value of cut 2 to 9 is taken into account. The growing mean forces F_c and F_{cN} can be explained by a changing cutting edge microgeometry and blunting of the cutting edge. For 42CrMo4, no significant change in the mean forces could be detected, whereas for hard-to-cut Inconel 718 the mean cutting force F_c was around 7 % lower for edge 2. The higher hardness in bigger distances to the build plate (see Fig. 1, edge 2) seems to increase the edges resistance to blunting. For the application in threading tools, which are also build up in vertical direction, the functional part should thus be positioned on the top relative to the build plate. As the force difference for Inconel 718 could be in the deviation range, further tests with a higher number of inserts should be conducted in the future.

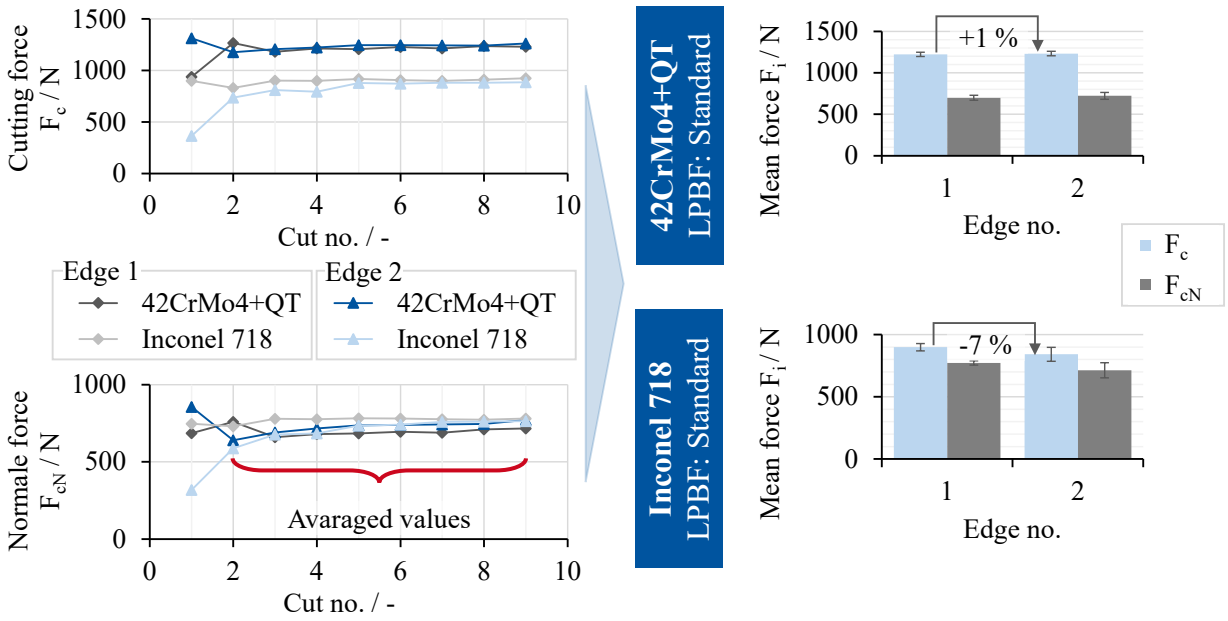

Fig. 4. Influence of build height onto force development (LPBF: Standard).

The LPBF parameter settings Standard and Productive did not influence the development and amplitude of the force signals for cutting of 42CrMo4 (Fig. 5). For cutting of Inconel 718, F_c and F_{cN} did grow along the number of cuts, with F_c being 11 % and F_{cN} 21 % higher for the insert produced with the productive LPBF parameters. The lower hardness of the productive parameters (see Fig. 1) led to a faster wear progression of the cutting edge in the hard-to-cut material even though forces for the standard parameters were comparable (F_{cN}) or lower (F_c).

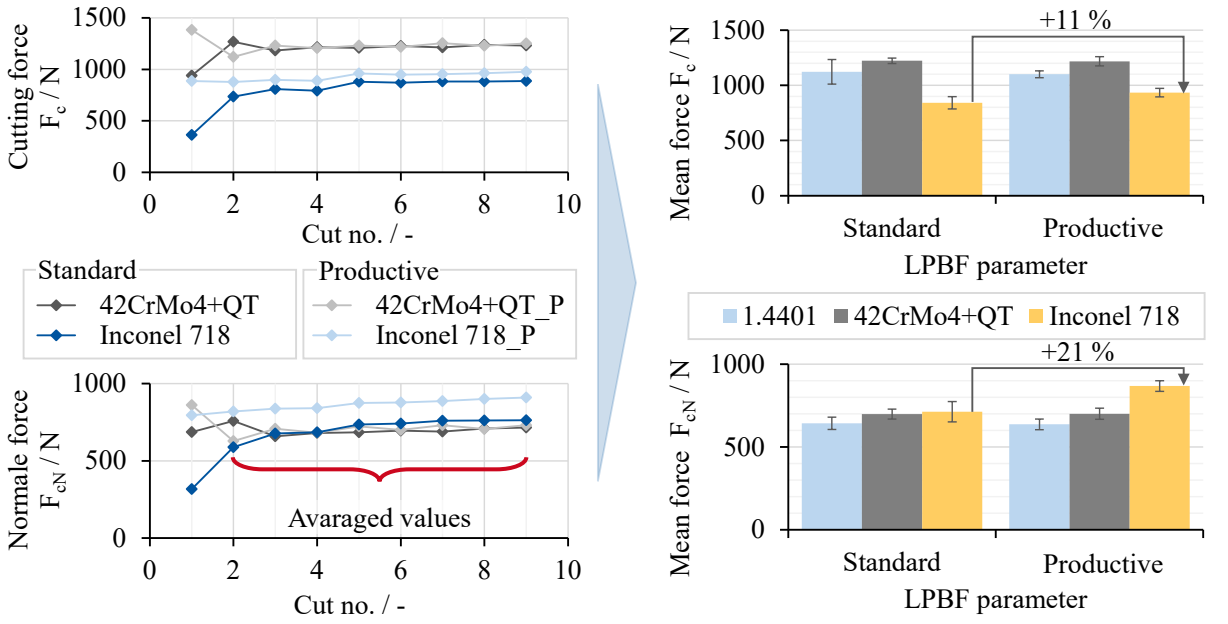

Fig. 5. Influence of LPBF parameter setting onto force development (1.4401: edge 1, 42CrMo4: edge 1, Inconel 718: edge 2).

A visual influence of the LPBF parameter setting and the build height on tool wear and cutting force progression for machining of 42CrMo4 could not be detected neither in the records of flank and rake face nor in the 3D scans, Fig. 6. A thermal influence, similar in size and shape and visible as an annealed rake face and flank face surface, was detected for all four inserts. The high thermal load can be explained by the high tensile strength of the quenched and tempered workpiece material. Chipping occurred on several inserts due to the high mechanical load and abrasive wear caused by the martensitic microstructure. The rising force amplitudes along the feed travel path l_f, which occurred during every cut, could not be explained by growing tool wear. The mean forces F_c and F_{cN} remained nearly constant along the number of cuts, see Fig. 4. A possible explanation might be the rising contact area between chip and rake face as visible in the high-speed video recording in Fig. 7 (42CrMo4+QT). Due to the rising chip up-curl radius, the contact length is constantly increasing, leading to more friction-induced force in and perpendicular to the direction of cut.

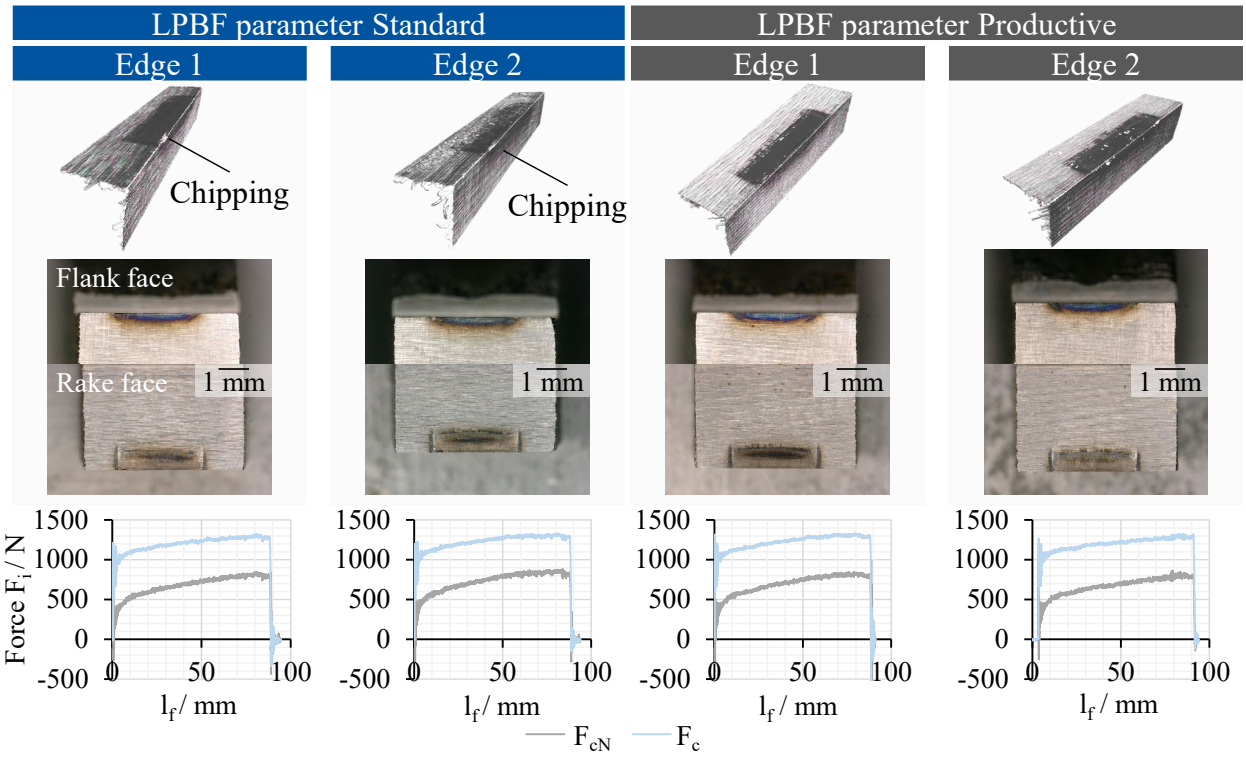

Fig. 6. Tool wear and force signal after nine consecutive cuts in 42CrMo4+QT.

Fig. 7 shows the chip formation captured by the high-speed camera as well as the resulting chip forms. 42CrMo4 exhibited a mainly continuous chip. In the first section of the chip, annealing colors were visible, indicating a high temperature evolution during cutting of the material. For 1.4401, mainly segmented chip formation occurred with material adhesions on the backside of the chip. CuZn21Si3P offered short, discontinuous chips due to the chipbreaking characteristics of the alloy elements. Cast iron GJL 250 with its brittle characteristics of the pearlite lamellae led to very short, dusty chips, whereas for Ti6Al4V a discontinuous lamellar chip formation was observed. Inconel 718 caused a thin, segmented chip with very regular chip up-curl radius.

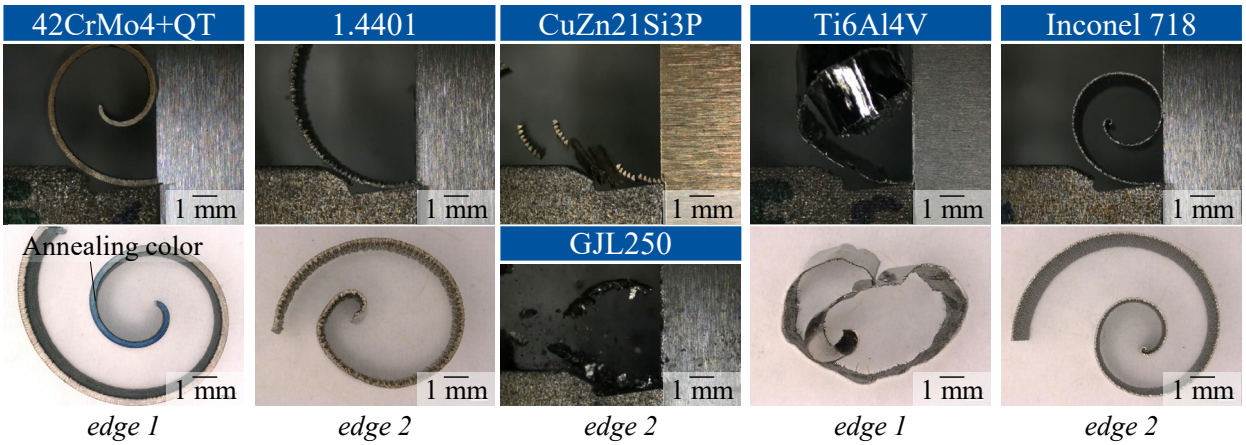

Fig. 7. Chip formation and chip form for all investigated materials (cut no. 3, LPBF: Standard).

As visible in Fig. 8, the forces F_c and F_{cN} did only grow significantly for hard-to-cut materials Inconel 718 and Ti6Al4V along the number of cuts. The cutting inserts seemed to withstand the mechanical load applied during the tool-workpiece-contact for all steel, cast and copper alloys.

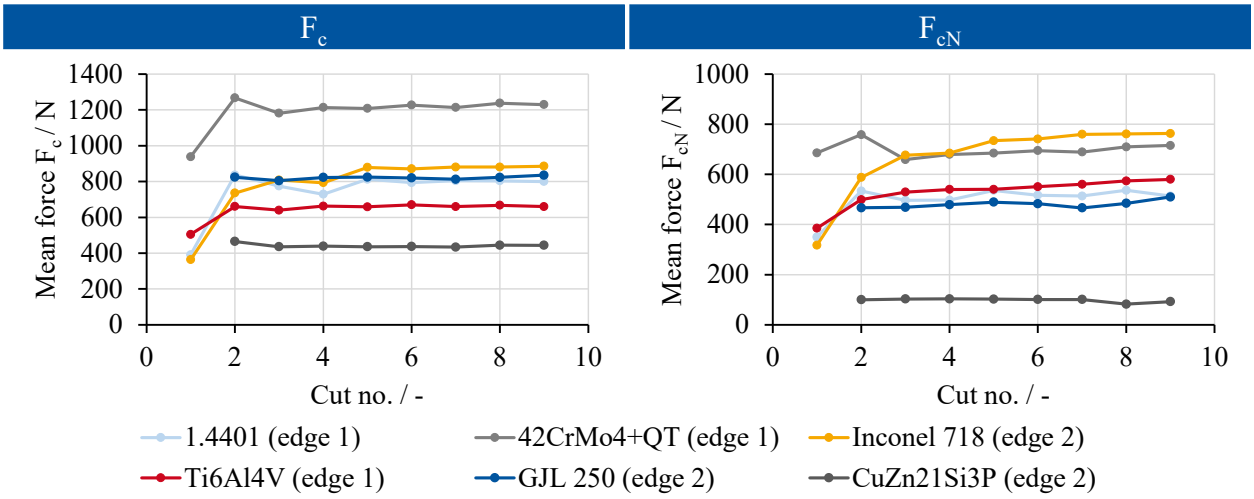

Fig. 8. Force growth along all number of cuts (LPBF: Standard).

The tool wear and force progression for all other materials is presented in Fig. 9. Adhering material could be detected on the rake face for cutting of 1.4401. The thermal load led to discolorations especially on the flank face for cutting of 1.4401 and Ti6Al4V caused by the low thermal conductivity of the materials. A relatively high flank wear was visible for Ti6Al4V and Inconel 718 due to high abrasive wear. The insert used for cutting of CuZn21Si3P appeared nearly unused after nine cuts, whereas strong material adhesions became visible on the flank and rake face for GJL 250. The continuous or discontinuous chip forms correlated with the force signal in terms of fluctuation. Especially for cutting of CuZn21Si3P and GJL 250, a high signal noise appeared in the force measurement, whereas for Inconel 718 nearly no fluctuations were detected.

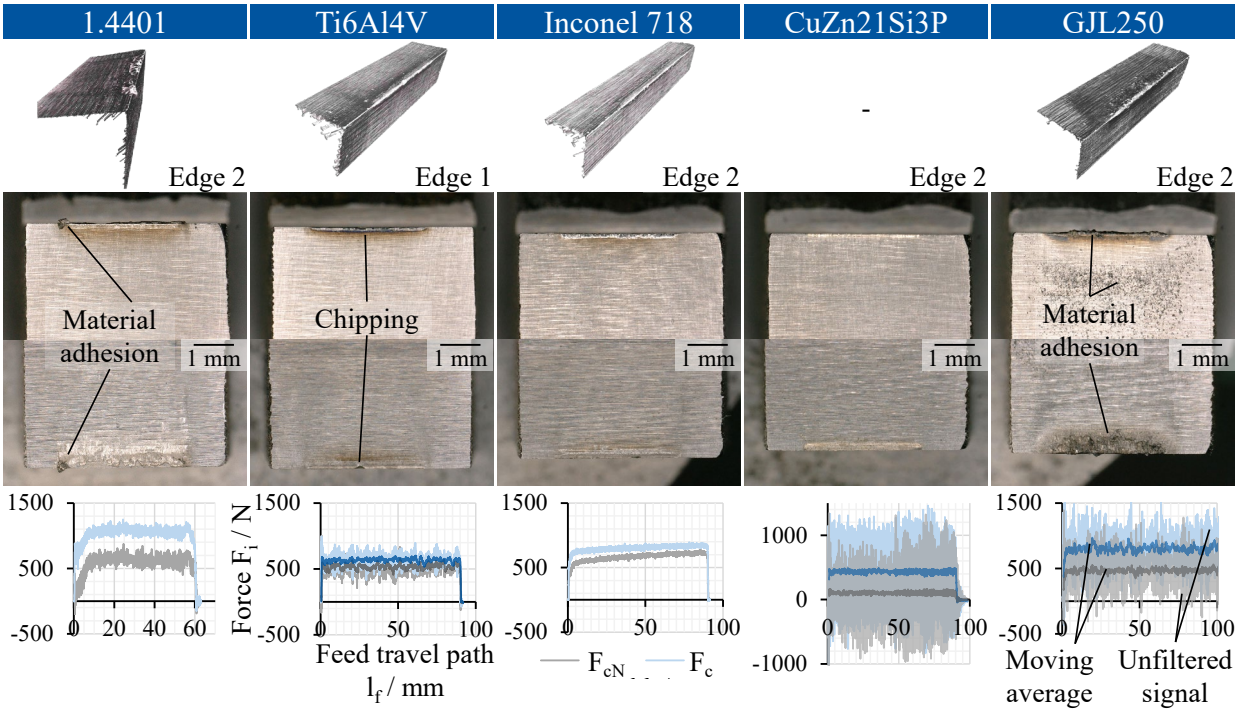

Fig. 9. Tool wear and force signal after nine consecutive cuts for different workpiece materials (LPBF: Standard).

Summary

All as-built, uncoated AM grooving inserts withstood the thermal and mechanical load during machining of the investigated materials within the scope of the experiments. The following findings were made:

- The hardness of the as-built test specimens varied along the distance to the build plate as well as between the two LPBF parameter settings with reduced hardness for small distances and productive LPBF parameters.
- The differences in the material properties of the cutting edge were negligible for machining of the steel alloys 42CrMo4+QT and 1.4401. An influence of the LPBF parameters and build height could be detected only during machining of Inconel 718 with a rising cutting force and cutting normal force over various cuts. The more productive LPBF parameter setting and a small distance to the build plate led to higher forces and faster tool wear development, respective faster tool wear rate of the cutting edge.
- For hard-to-cut materials Inconel 718 and Ti6Al4V, the cutting force rose over various cuts. Chipping phenomena appeared for cutting of Ti6Al4V, whereas high thermal loads resulting in discoloration on the tool flank and rake face, as well as on the chip surface occurred for cutting of 42CrMo4+QT. Adhesion phenomena on the rake face could be detected for alloyed steel 1.4401.

The findings show the capabilities of AM tools made from HS6-5-3-8 even in hard-to-cut materials. As only a limited amount of cuts was performed, tool wear development and thus tool life should be closer analyzed in future investigations, taking into account long-term phenomena. Based on these results, the use of coatings for the AM processed HSS substrate appears reasonable. Thus, thermal influences and material adhesion can be reduced. In future works, the influence of a heat treatment on microstructure and mechanical properties of the AM HSS will be analyzed and compared to conventionally manufactured HSS. In a next step, AM threading tools manufactured from HS6-5-3-8 will be investigated, using the geometrical freedom for an adapted channel and

outlet nozzle design of the internal cutting fluid supply, extending tool life and reducing scrap parts. Another possible application for additively processed HSS can be the manufacturing or repairing of AM broaching tools.

Acknowledgements
The IGF-research project 21581 N (Acronym: “AddBo”) of the Forschungsgemeinschaft Werkzeuge und Werkstoffe e.V. (FGW) is funded by the AiF within the program to promote joint industrial research (IGF) by the Federal Ministry for Economic Affairs and Climate Action (BMWK), following a decision of the German Bundestag. The LPBF manufactured parts within the research project were provided by the Fraunhofer Institute for Laser Technology (ILT) in Aachen, Germany with kind support from Tim Lücke. The authors would like to thank the companies Deutsche Edelstahlwerke Specialty Steel GmbH & Co. KG and Meyer + Dörner Räumwerkzeuge GmbH for their support within the project.

References
[1] T. Scherer, Beanspruchungs- und fertigungsgerechte Gestaltung additiv gefertigter Zerspanwerkzeuge, Dissertation, TU Darmstadt, Darmstadt, 2020.
[2] F.A.M. Vogel, S. Berger, E. Özkaya, D. Biermann, Vibration Suppression in Turning TiAl6V4 Using Additively Manufactured Tool Holders with Specially Structured, Particle Filled Hollow Elements, Procedia Manuf. 40 (2019) 32-37. https://doi.org/10.1016/j.promfg.2020.02.007
[3] T. Lakner, High-pressure cutting fluid supply in milling, Dissertation, RWTH Aachen University, Aachen, 2021.
[4] Dr. Mapal, K.G. Kress, Lasersintern erweitert Fertigungsmöglichkeiten von Präzisionswerkzeugen, Diamond Business, 2017.
[5] A.G. Urma Werkzeugfabrik, Serien-Drehwerkzeug mit innenliegenden Kanalstrukturen, Maschinenbau Schweiz No. 11 (2019) 14-15.
[6] T. Kulmala, Geringeeres Gewicht - höhere Leistung, 2019. Available: https://www.sandvik.coromant.com/de-de/mww/pages/t_cm390am.aspx. (accessed 20 July 2020).
[7] M. Padmakumar, Additive Manufacturing of Tungsten Carbide Hardmetal Parts by Selective Laser Melting (SLM), Selective Laser Sintering (SLS) and Binder Jet 3D Printing (BJ3DP) Techniques, Laser. Manuf. Mater. Process. 7 (2020) 338-371. https://doi.org/10.1007/s40516-020-00124-0
[8] B.D. Kernan, E.M. Sachs, M.A. Oliveira, M.J. Cima, Three-dimensional printing of tungsten carbide-10wt% cobalt using a cobalt oxide precursor, Int. J. Refract. Metal. Hard Mater. 25 (2007) 82-94. https://doi.org/10.1016/j.ijrmhm.2006.02.002
[9] T. Schwanekamp, Pulverbettbasiertes Laserstrahlschmelzen von Hartmetallen zur additiven Herstellung von Zerspanwerkzeugen, Dissertation, Ruhr-Universität Bochum, 2021. https://doi.org/10.13154/294-7802
[10] M. Weigold, T. Scherer, E. Schmidt, M. Schwentenwein, T. Prochaska, Additive Fertigung keramischer Schneidstoffe, wt Werkstattstechnik online 110 (2020) 2-6.
[11] J. Saewe, C. Gayer, A. Vogelpoth, J.H. Schleifenbaum, Feasability Investigation for Laser Powder Bed Fusion of High-Speed Steel AISI M50 with Base Preheating System, BHM Berg- und Hüttenmännische Monatshefte 164 (2019) 101-107. https://doi.org/10.1007/s00501-019-0828-y
[12] F. Klocke, Manufacturing Processes 1: Cutting, Springer, Berlin, Heidelberg, 2011.
[13] Wohlers Associates, Wohlers Report 2022: 3D printing and additive manufacturing global state of the industry, Wohlers Associates, Fort Collins (Colorado), 2022.
[14] K. Kempen, B. Vrancken, S. Buls, L. Thijs, J. van Humbeeck, J.-P. Kruth, Selective Laser Melting of Crack-Free High Density M2 High Speed Steel Parts by Baseplate Preheating, J. Manuf. Sci. Eng. 136 (2014). https://doi.org/10.1115/1.4028513

[15] L. Zumofen, C. Beck, A. Kirchheim, H.-J. Dennig, Quality Related Effects of the Preheating Temperature on Laser Melted High Carbon Content Steels, Industrializing Additive Manufacturing - Proceedings of Additive Manufacturing in Products and Applications - AMPA2017 (2018) pp. 210-219. https://doi.org/10.1007/978-3-319-66866-6_21